ADVANCED FUNCTIONAL MATERIALS
www.afm-journal.de

Materials Views
www.MaterialsViews.com

Organic Light-Emitting Diodes with 30% External Quantum Efficiency Based on a Horizontally Oriented Emitter

*Sei-Yong Kim, Won-Ik Jeong, Christian Mayr, Young-Seo Park, Kwon-Hyeon Kim, Jeong-Hwan Lee, Chang-Ki Moon, Wolfgang Brütting, and Jang-Joo Kim**

High-efficiency phosphorescent organic light-emitting diodes (OLEDs) doped with $Ir(ppy)_2(acac)$ [bis(2-phenylpyridine)iridium(III)-acetylacetonate] in an exciplex forming co-host have been optically analyzed. This emitter has a preferred orientation with the horizontal to vertical dipole ratio of 0.77:0.23 as compared to 0.67:0.33 in the isotropic case. Theoretical analysis based on the orientation factor (Θ, the ratio of the horizontal dipoles to total dipoles) and the photoluminescence quantum yield (q_{PL}) of the emitter predicts that the maximum external quantum efficiency (EQE) of the OLEDs with this emitter is about 30%, which matches very well with the experimental data, indicating that the electrical loss of the OLEDs is negligible and the device structure can be utilized as a platform to demonstrate the validity of optical modeling. Based on the results, the maximum EQE achievable for a certain emitting dye in a host can be predicted by just measuring q_{PL} and Θ in a neat film on glass without the need to fabricate devices, which offers a universal plot of the maximum EQE as a function of q_{PL} and Θ.

1. Introduction

Organic light-emitting diodes (OLEDs) with horizontally aligned emitters have the potential to achieve high external quantum efficiency (EQE) without out-coupling enhancement layers. An emitter with a horizontal transition dipole moment results in a much higher out-coupling efficiency than the vertically aligned dipole as demonstrated in polymers and vacuum-evaporated organic molecules.[1–10] Recently, not only fluorescent molecules but also some phosphorescent dyes are reported to have preferred horizontal dipoles where a high EQE of over 30% is expected.[11–15] Unfortunately no experimental data have yet demonstrated the potential of horizontally oriented phosphorescent dyes to attain efficiencies over 30%, to the best of our knowledge, because of the problems associated with obtaining a device structure that shows a perfect electron and hole balance. Moreover, the most commonly used green phosphorescent dye, $Ir(ppy)_3$, doped in *N,N*′-dicarbazolyl-4,4′-biphenyl (CBP) was reported to have an isotropic distribution of emitting dipoles.[15] Thus, it is important to develop or find a host/guest system that has preferentially horizontal dipoles as well as a device structure with nearly 100% charge balance, that means without electrical loss, to demonstrate the validity of the prediction of the optical model.

Recently our group reported a very high efficiency green phosphorescent OLED with an EQE of 29.1% and an extremely low roll-off efficiency at high current density.[16] In this device $Ir(ppy)_2(acac)$ [bis(2-phenylpyridine)iridium(III)-acetylacetonate] was doped in the exciplex forming co-host system of TCTA [4,4′,4″-tri (*N*-carbazolyl) triphenylamine] and [bis-4,6-(3,5-di-3-pyridylphenyl)-2-methylpyrimidine] (B3PYMPM). The high efficiency of this OLED with low roll-off efficiency indicates that the electrical loss (including charge balance and exciton-polaron quenching) seems to be negligible in the device so that it can be used as a platform to analyze the out-coupling efficiency and the factors influencing the EQE and eventually validate the prediction of an optical model.

In this paper, we demonstrate by optical analysis that the phosphorescent emitter $Ir(ppy)_2(acac)$ in the device has a preferred non-isotropic orientation with a horizontal to vertical dipole ratio of 0.77:0.23 (Θ = 0.77), and the device has a maximum EQE of 30% based on the photoluminescence (PL) quantum yield (q_{PL}) of 0.94 in the thin film and 100% charge balance. The theoretical prediction agrees very well with the experimental data, validating the optical model used for the prediction of the EQE. Based on this validation, we offer a universal plot of maximum efficiency achievable with different values of q_{PL} and Θ in a dye-doped emission layer (EML) without the need for fabricating devices. The optical analysis indicates that OLEDs with an EQE higher than 40% can be realized without any extra light extraction layers, if phosphorescent dyes with q_{PL} and Θ over 95% are used.

Dr. S.-Y. Kim, Dr. W.-I. Jeong, Dr. Y.-S. Park, K.-H. Kim, J.-H. Lee, C.-K. Moon, Prof. J.-J. Kim
Department of Materials Science and Engineering and Center for Organic Light Emitting Diode
Seoul National University
Seoul 151-742, South Korea
E-mail: jjkim@snu.ac.kr
C. Mayr, Prof. W. Brütting
Institute of Physics
University of Augsburg
86135 Augsburg, Germany

DOI: 10.1002/adfm.201300104

2. Simulation of External Quantum Efficiency

The EQE of an OLED is expressed by the following equation:[17]

$$\eta_{\mathrm{EQE}} = \gamma \times \eta_{\mathrm{S/T}} \times q_{\mathrm{PL}} \times \eta_{\mathrm{out}} \quad (1)$$

where γ is the charge balance factor, $\eta_{S/T}$ is the singlet-triplet factor ($\eta_{S/T} = 0.25$ for fluorescent, $\eta_{S/T} = 1$ for phosphorescent emitters), q_{PL} is the PL quantum yield, and η_{out} is the out-coupling efficiency of the emitted light. However, the quantum efficiency of an emitter in a micro-cavity structure is influenced by the orientation of the emitter, the local electric field at the dipole position, and the proximity to a metal layer. The η_{out} is influenced not only by the device structure but also by the orientation of the emitting dipoles so that the EQE must be modified as follows:[15,18]

$$\eta_{\mathrm{EQE}} = \gamma \times \eta_{\mathrm{S/T}} \times q_{\mathrm{eff}}(q_{\mathrm{PL}}, \Theta, \Gamma) \times \eta_{\mathrm{out}}(\Theta, \Gamma) \quad (2)$$

where q_{eff} is the effective quantum yield that describes the probability of radiative exciton decay in an optical cavity structure (i.e., the Purcell effect[19]), which generally depends on q_{PL},Θ, and the geometric factor of the device (Γ) including the device structure and the location of the emission zone in the device.[12,13,15] In a similar manner, η_{out} is influenced by Θ and Γ.[11,15,20] The γ value is often assumed to be unity in state-of-the-art OLEDs, however, this value is not a constant but a fitting parameter in this study. With separately measured values of q_{PL} and Θ, and using known information of the device structure, we can now calculate q_{eff} and η_{out} from a classical dipole model[21,22] and then fit this to the experimentally obtained EQE to extract γ. Therefore, we can exactly analyze the effect of the emitter orientation, the electrical loss, as well as the device structure by fitting theoretically predicted EQE to experimental data. Details of the method for calculating η_{out} were described elsewhere.[20,23] We assumed that the emission zone is located in the middle of the EML of the OLEDs, which is a reasonable assumption for the device having a uniformly distributed profile of the emission zone such as the co-host system used here.[24]

A schematic diagram of the device structure and the chemical structure of the materials used in this study are shown in **Figure 1**a. The refractive indices of the organic layers, except for B3PYMPM, were measured by a spectroscopic ellipsometer.[25] The refractive indices of B3PYMPM, the glass substrate, the indium tin oxide (ITO) layer, and metal are taken from the literature.[9,26,27] The refractive indices of the undoped co-host layer (TCTA:B3PYMPM, 1:1 molar ratio) measured by a spectroscopic ellipsometer are displayed in Figure 1b. We ignored the modification of the optical constant by the doping of the

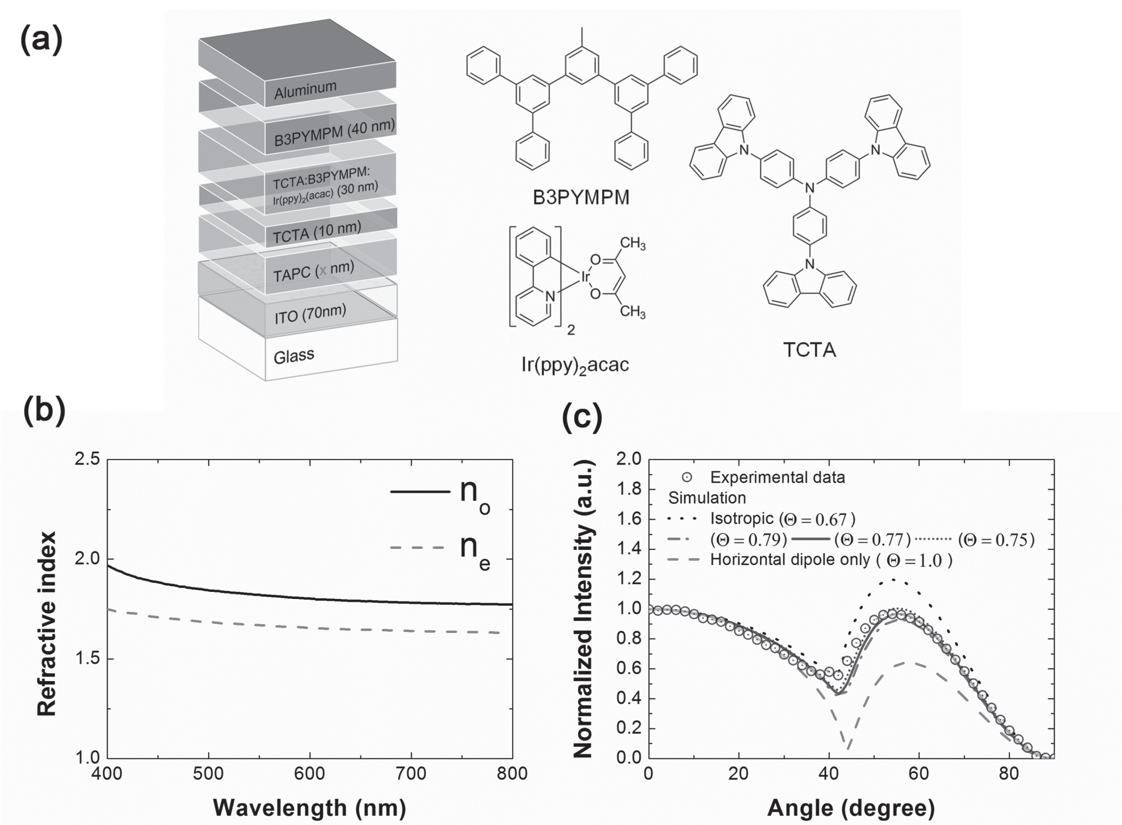

Figure 1. a) Schematic diagram of the device and molecular structures of co-host and a phosphorescent dye used in this study. The thickness of the1,1-bis(di-4-tolylaminophenyl)cyclohexane (TAPC) layer was varied from 40 to 100 nm. b) Refractive indices of undoped co-host layer (TCTA:B3PYMPM, 1:1 of molar ratio) measured by a variable angle spectroscopic ellipsometer. c) Experimentally obtained angle-dependent PL spectrum of the EML on fused silica substrate (circle) compared to simulated spectra (lines) with a different ratio of horizontal dipoles (Θ) (dashed line for $\Theta = 1$ (fully horizontal), dashed-dotted line for $\Theta = 0.79$, thick-solid line for $\Theta = 0.77$, short-dotted line for $\Theta = 0.75$, and dotted line for $\Theta = 0.67$ (isotropic)).

phosphorescent dye molecules because of the low doping concentration (<10%). The optical constants of the co-host system show strong anisotropy with an ordinary refractive index (n_o) of 1.8342 and an extra-ordinary refractive index (n_e) of 1.6776 at a wavelength of 520 nm. The strong optical anisotropy indicates that the host materials are horizontally oriented.

3. Determination of Emitter Orientation

The dipole orientation of the emitting dyes in the host matrix was determined from the analysis of the angle-dependent PL spectrum of the EML.[28] The sample was prepared by co-depositing B3PYMPM, TCTA, and $Ir(ppy)_2(acac)$ in the same molar ratio of the host materials and 8 wt% of the dopant on a pre-cleaned 1 mm-thick fused silica substrate. The thickness of the film was 30 nm, which corresponds to the thickness of the EML in the OLED. A He-Cd laser (325 nm) was used as the excitation source of the sample and the *p*-polarized emitted light at 520 nm, corresponding to the peak wavelength of the PL spectrum of the phosphorescent dye, was detected. For the simulation of the angle-dependent PL spectrum, the optical anisotropy was accommodated in the model by using the effective refractive index as a function of the propagation direction of the *p*-polarized emitted light. The effective refractive index (n_{eff}) is defined as a function of the emission angle (θ) in the organic layer as follows:

$$\frac{1}{n_{\mathrm{eff}}^2} = \frac{\cos^2\theta}{n_o^2} + \frac{\sin^2\theta}{n_e^2} \tag{3}$$

The effective refractive index of the organic layer for the *p*-polarized light changes from n_o to n_e as the angle of emission varies from 0° to 90°. The experimental data and the simulation results of the angle-dependent PL spectrum of the 30-nm thick $Ir(ppy)_2(acac)$ doped TCTA:B3PYMPM film are shown in Figure 1c. The experimental data fit well with the horizontal to vertical dipole ratio of 0.77:0.23, indicating that the emitter in the EML has more horizontally oriented dipoles than vertically oriented ones compared to the isotropic orientation and the result is consistent with the previous report.[14] It is interesting to note that the Θ value is the same as that of bis(2-methyldibenzo[f,h]quinoxaline) (acetylacetonate) iridium (III) ($Ir(MDQ)_2(acac)$).[11–13]

4. Efficiency of OLEDs

The device under investigation has a simple structure of glass/ITO (70 nm)/TAPC (x nm)/TCTA (10 nm)/TCTA:B3PYMPM:$Ir(ppy)_2(acac)$ (1:1 molar ratio and 8 wt%) (30 nm)/B3PYMPM (40 nm)/Al (100 nm), where TAPC represents 1,1-bis(di-4-tolylaminophenyl)cyclohexane. The thickness of the TAPC layer was set as a parameter and varied from 40 to 100 nm.

The current density–voltage–luminance (*J*–*V*–*L*) characteristics of the devices with different thicknesses of the TAPC layer are shown in **Figure 2**a. The *J*–*V* characteristics of all the devices are not significantly different from each other, especially in the low current region, due to a high hole mobility of TAPC (ca. 10^{-2} cm^2 V^{-1} s^{-1}).[29] Thus, the difference in

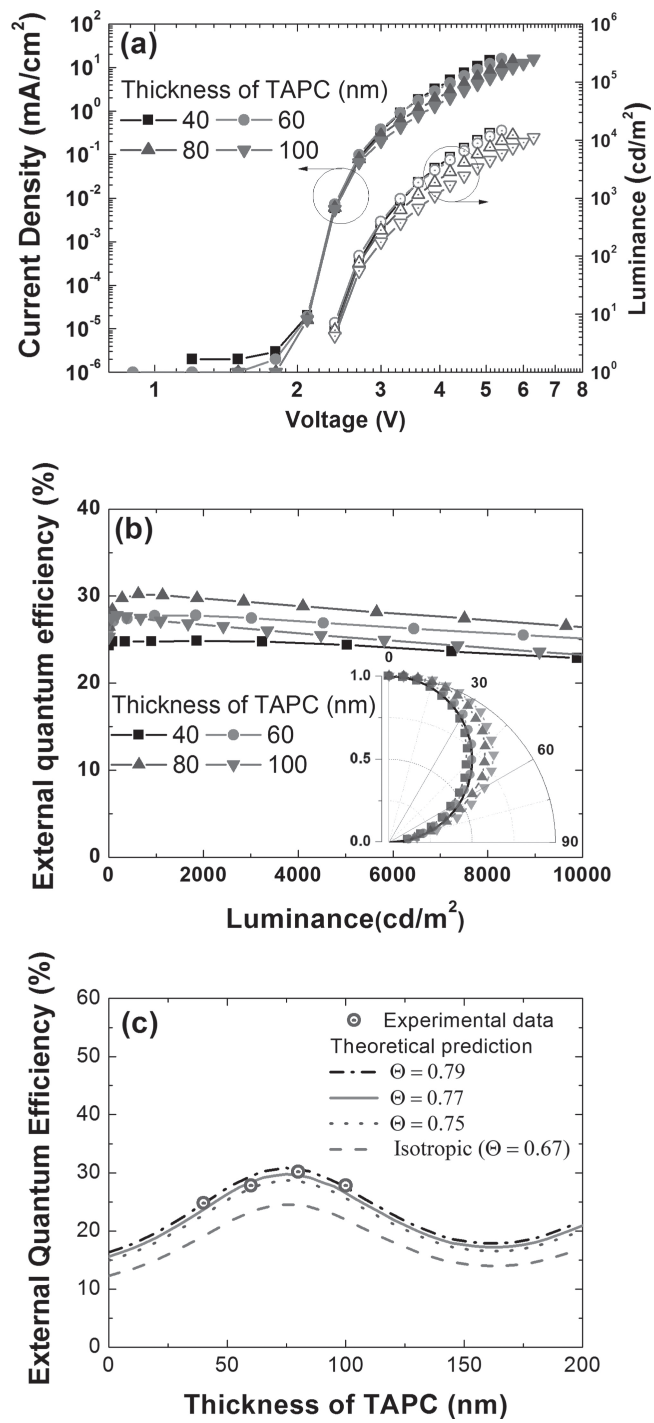

Figure 2. The experimental data of the OLEDs with different thicknesses of TAPC layer (40, 60, 80 and 100 nm): a) Current density–voltage–luminance curves. b) EQE vs. luminance (inset: angle-dependent emission patterns of the OLEDs. The solid line indicates the Lambertian distribution).c) Experimental EQEs (circles) are compared with simulated EQEs with different orientation factors of the dipoles; dashed-dotted line for $\Theta = 0.79$, solid line for $\Theta = 0.77$, dotted line for $\Theta = 0.75$, and dashed line for $\Theta = 0.67$ (isotropic). A q_{PL} of 0.94 and γ of 1.0 were used for the simulation.

the efficiency of the OLEDs with different thicknesses of the TAPC layer originates mostly from an optical effect. The turn-on voltages of all the devices are identical at 2.4 V and the

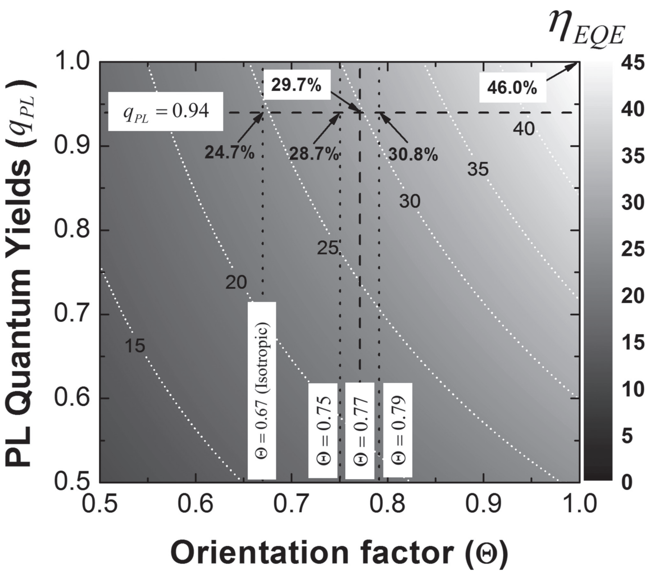

Figure 3. Contour plot of the simulation results of EQE as a function of q_{PL} and Θ. The device structure shown in Figure 1 with TAPC thickness of 75 nm was used for the simulation. The two dashed lines indicate the locus of the EQE for $\Theta = 0.77$ and $q_{PL} = 0.94$, respectively. In a similar manner, the dotted lines indicate the EQE for $\Theta = 0.67$ (isotropic), 0.75, and 0.79, respectively.

driving voltages of the devices are less than 3.9 V and 6.3 V for 1000 and 10000 cd m^{-2}, respectively. The maximum current efficiency and power efficiency were 106 cd A^{-1} (60 nm-thick TAPC) and 127.3 lm W^{-1} (80 nm-thick TAPC), respectively (not shown). The EQE of the devices corrected for their emission patterns are displayed in the inset of Figure 2b. The maximum EQE (30.2%) was obtained with the 80 nm-thick TAPC layer. To the best of our knowledge, this EQE value is the highest one for bottom-emitting green phosphorescent OLEDs based on an ITO electrode. There is a paper reporting an EQE of 29.2% and 93 cd A^{-1} using the same emitter.[30] Unfortunately, the authors of this work did not take into account emitter orientation, which is obviously the key to achieve higher EQE values. The measured EQE values of the devices are plotted in Figure 2c against the thickness of the TAPC layer.

Optical simulation of the EQE of the devices was performed using the experimentally obtained values of $q_{PL} = 0.94$ and $\Theta = 0.77 \pm 0.02$. The PL quantum yield was measured using an integrating sphere[23,31] and the sample consisted of a 50-nm thick emitting layer (TCTA:B3PYMPM:Ir(ppy)$_2$(acac), 1:1 molar ratio and 8 wt%) on a quartz substrate. The experimental results are very well described by the simulated results as shown in Figure 2c under the condition of $\gamma = 1$ as well as $\eta_{S/T} = 1$ (see Equation 2), indicating that the electrical loss is indeed negligible. In other words, the injected electrons and holes into the EML of the OLEDs efficiently recombine to form excitons that are allowed to decay radiatively. The excellent match between the experimental and the simulation results clearly indicates that the optical simulation describes the maximum achievable EQE for the known values of q_{PL} and Θ when the device structure is optimized electrically and optically. This fact implies that we can predict the maximum EQE achievable for a certain emitting dye in a host by just measuring the q_{PL} and Θ on a neat film of the EML on glass without the need for fabricating full OLED devices.

Based on this idea, we extend the simulation to calculate the maximum achievable EQEs as a function of q_{PL} and Θ. The corresponding simulation results are shown in **Figure 3** as a contour plot. We used the structure shown in Figure 1a with the optimized thickness of the TAPC layer (75 nm) for the simulation. The maximum efficiency increases as q_{PL} and Θ approach 1 as expected. Surprisingly, a maximum EQE of 46% can be achieved in normal ITO-based bottom-emitting OLEDs without any extra outcoupling layers using a phosphorescent dye with $q_{PL} = 1$ and $\Theta = 1$. Practically an EQE of over 40% is possible with $q_{PL} = 0.95$ and $\Theta = 0.95$. In contrast, the maximum EQE of an OLED with isotropically oriented phosphorescent dyes is much lower (ca. 25%).

5. Conclusions

Optical analysis of our high-efficiency OLED showed that the phosphorescent dye Ir(ppy)$_2$(acac) in the EML has a preferred horizontal dipole orientation (parallel to the substrate plane), which results in a maximum EQE of 30% providing there are negligible electrical losses in the device. The prediction matches very well with the experimental value, suggesting that the device has almost perfect electron–hole balance and the classical dipole model used for the calculation of q_{eff} and η_{out} are valid for the analysis of the performance of OLEDs. The analysis indicates that an EQE of 40% is possible in ITO-based bottom-emitting OLEDs without any extra light extraction layers.

6. Experimental Section

Device Fabrication: The OLEDs were fabricated by thermal evaporation onto cleaned glass substrates pre-coated with ITO. Prior to the deposition of the organic layers, the ITO substrates were exposed to UV-ozone flux for 10 min following degreasing in acetone and isopropyl alcohol. All the layers were grown by thermal evaporation at a base pressure of $<5 \times 10^{-7}$ Torr without breaking the vacuum.

Measurement of Angle-Dependent PL Intensity: The experimental setup was composed with a motorized rotation stage, a fused silica-based half cylindrical lens with a sample holder, a dichroic mirror to filter the excitation beam, a polarizer to classify the polarity of the emitted light, a fiber-guided detector combined with a monochromator and a photomultiplier tube. A continuous-wave He:Cd laser (325 nm, Mellisgriot Co.) was used as the excitation source of the sample and the incident angle was 45°. The *p*-polarized emitted light at 520 nm, corresponding to the peak wavelength of the PL spectrum of the phosphorescent dye, was detected.

Characterization of the OLEDs: The current density, the luminance, and the EL spectra were measured using a Keithley 2400 source meter and a SpectraScan PR650 (Photo Research). The angular distribution of the EL intensity was measured using a Keithley 2400 source meter, a rotation stage, and an Ocean Optics S2000 fiber optic spectrometer. The EQE and the power efficiency of the OLEDs were calculated from the current density, the luminance, the EL spectra, and the angular distribution of the EL intensity.

Measurement of PL Quantum Yield of the Emitter: The PL efficiency of the emitter was measured using an integrating sphere (Labsphere Co., 6 inches in diameter). A He:Cd laser (325 nm) was used as the excitation source (the same as the one used for the measurement of the

FULL PAPER

angle-dependent PL intensity). A monochromator (Acton Research Co.) attached to a photomultiplier tube (Hamamatsu Photonics K.K.) was used as the optical detector system. To avoid degradation of the samples by laser excitation, the samples were kept in an inert environment by blowing nitrogen gas into the integrating sphere.

Acknowledgements

This work was supported by the industrial strategic technology development program [10035225, development of core technology for high performance AMOLED on plastic] funded by MKE/KEIT of Korea. C.M. acknowledges financial support by the Deutscher Akademischer Austauschdienst (DAAD) and Bayerische Forschungsstiftung (BFS).

Received: January 10, 2013
Revised: February 17, 2013
Published online: March 27, 2013

[1] J.-S. Kim, P. K. H. Ho, N. C. Greenham, R. H. Friend, *J. Appl. Phys.* **2000**, *88*, 1073.
[2] P. K. H. Ho, J.-S. Kim, J. H. Burroughes, H. Becker, S. F. Y. Li, T. M. Brown, F. Cacialli, R. H. Friend, *Nature* **2000**, *404*, 481.
[3] L. H. Smith, J. A. E. Wasey, I. D. W. Samuel, W. L. Barnes, *Adv. Funct. Mater.* **2005**, *15*, 1839.
[4] J. M. Ziebarth, M. D. McGehee, *J. Appl. Phys.* **2005**, *97*, 064502.
[5] M. Flämmich, M. C. Gather, N. Danz, D. Michaelis, A. H. Brauer, K. Meerholz, A. Tunnermann, *Org. Electron.* **2010**, *11*, 1039.
[6] H.-W. Lin, C.-L. Lin, H.-H. Chag, Y.-T. Lin, C.-C. Wu, Y.-M. Chen, R.-T. Chen, Y.-Y. Chien, K.-T. Wong, *J. Appl. Phys.* **2004**, *95*, 881.
[7] H.-W. Lin, C.-L. Lin, C.-C. Wu, T.-C. Chao, K.-T. Wong, *Org. Electron.* **2007**, *8*, 189.
[8] D. Yokoyama, A. Sakaguchi, M. Suzuki, C. Adachi, *Org. Electron.* **2009**, *10*, 127.
[9] D. Yokoyama, H. Sasabe, Y. Furukawa, C. Adachi, J. Kido, *Adv. Funct. Mater.* **2011**, *21*, 1375.
[10] J. Frischeisen, D. Yokoyama, A. Endo, C. Adachi, W. Brütting, *Org. Electron.* **2011**, *12*, 809.
[11] M. Flämmich, J. Frischeisen, D. S. Setz, D. Michaelis, B. C. Krummacher, T. D. Schmidt, W. Brütting, N. Danz, *Org. Electron.* **2011**, *12*, 1663.
[12] T. D. Schmidt, D. S. Setz, M. Flämmich, J. Frischeisen, D. Michaelis, B. C. Krummacher, N. Danz, W. Brütting, *Appl. Phys. Lett.* **2011**, *99*, 163302.
[13] L. Penninck, F. Steinbacher, R. Krause, K. Neyts, *Org. Electron.* **2012**, *13*, 3079.
[14] P. Liehm, C. Murawski, M. Furno, B. Lüssem, K. Leo, M. C. Gather, *Appl. Phys. Lett.* **2012**, *25*, 253304.
[15] W. Brütting, J. Frischeisen, T. D. Schmidt, B. J. Scholz, C. Mayr, *Phys. Status Solidi A* **2013**, *210,* 44.
[16] Y.-S. Park, S. Lee, K.-H. Kim, S.-Y. Kim, J.-H. Lee, J.-J. Kim, unpublished.
[17] T. Tsutsui, E. Aminaka, C. P. Lin, D. U. Kim, *Philos. Trans. R. Soc. A* **1997**, *355*, 801.
[18] M. Furno, R. Meerheim, S. Hofmann, B. Lüssem, K. Leo, *Phys. Rev. B* **2012**, *85*, 115205.
[19] E. M. Purcell, *Phys. Rev.* **1946**, *69*, 681.
[20] S. Y. Kim, J. J. Kim, *Org. Electron.* **2010**, *11*, 1010.
[21] R. R. Chance, A. Prock, R. Silbey, *Molecular Fluorescence and Energy Transfer Near Interfaces*, John Wiley & Sons, Inc., New York **1978**.
[22] J. A. E. Wasey, W. L. Barnes, *J. Mod. Opt.* **2000**, *47*, 725.
[23] W. I. Jeong, S. Y. Kim, J. W. Kang, J. J. Kim, *Chem. Phys.* **2009**, *355*, 25.
[24] J. Lee, J. I. Lee, J. Y. Lee, H. Y. Chu, *Org. Electron.* **2009**, *10*, 1529.
[25] Refractive indices were measured by the KRISS (Korea Research Institute of Standards and Science).
[26] E. D. Palik, G. Ghosh, *Handbook of Optical Constants of Solids*, Academic Press, San Diego, CA **1998**.
[27] R. A. Synowicki, *Thin Solid Films* **1998**, *313*, 394.
[28] J. Frischeisen, D. Yokoyama, C. Adachi, W. Brütting, *Appl. Phys. Lett.* **2010**, *96*, 073302.
[29] P. M. Borsenberger, L. Pautmeier, R. Richert, H. Bassler, *J. Chem. Phys.* **1991**, *94*, 8276.
[30] M. G. Helander, Z. B. Wang, J. Qiu, M. T. Greiner, D. P. Puzzo, Z. W. Liu, Z. H. Lu, *Science* **2011**, *332*, 944.
[31] J. C. de Mello, H. F. Witmann, R. H. Friend, *Adv. Mater.* **1997**, *9*, 230.